# Chapter 5

# ELECTRON COLLISION WITH FLUORONITRILES

*In this chapter, we provide the findings from our studies on electron-driven molecular events for the fluoronitriles $C_3F_5N$ and $C_4F_7N$ over a large energy range, from the ionization potential to 5000 eV. We use SCOP, CSP-ic and 2P-SEM techniques to estimate elastic and inelastic effects. The research encompasses multiple correlations, predicting dipole polarizability, determining the dielectric constant, and calculating the number density N for these fluoronitriles.*

## 5.1 Introduction

As an insulating gas, sulphur hexafluoride ($SF_6$) is commonly used in high-voltage devices [1]. Non-toxicity, a low boiling point, and excellent insulating performance are just a few of the many physicochemical features of $SF_6$ that lead in this direction. However, $SF_6$ does not decompose very quickly in the atmosphere and has a GWP that is 22,800 times higher than that of carbon dioxide. Thus, finding a suitable alternative to $SF_6$ has become one of the most critical issues in high-voltage mechatronics. Because of its high reliability, low electromagnetic radiation, $SF_6$ insulated equipment is widely utilised in high and ultra-high- electricity voltage systems. However, there would be a significant economic loss if insulation on equipment failed. This has also prompted the search for potential $SF_6$ replacements. The fluoronitrile ($C_3F_5N$ and $C_4F_7N$) gases, have been studied intensively [2–4] in recent years as a potential alternative to $SF_6$.

Thus, fluoronitriles have low GWP and high dielectric strength compared to $SF_6$, which makes them most suitable alternative to $SF_6$ in various applications. Table 5.2 compares the dielectric strength and GWP of $SF_6$ and fluoronitrile gases.

However, there has been comparatively less research into microscopic parameters such the ionisation cross sections ($Q_{ion}$) upon electron impact. This $Q_{ion}$ is a key variable in the study of electron avalanche and gas breakdown mechanisms [5,6].

Gas electron transport coefficients and discharge reaction rates can be calculated using either Boltzmann's computations or Monte-Carlo calculations [5,6], with $Q_{ion}$ serving as an input. $Q_{ion}$ can be measured experimentally, although not for every gas due to the difficulty of the measurements owing to the molecules' reactivity, Theoretical methods become potent tools for obtaining $Q_{ion}$, which might be used as a reference in the investigation of the insulating properties of gases. CSP-ic technique [7], Binary-Encounter Bethe (BEB) method [8], and Deutsch-Mark (DM) method [9] are the most well-known theoretical approaches.

Our group has developed a CSP-ic technique [10], which is used in the present work to calculate the $Q_{ion}$ for the molecules of interest in the present work.

Constructing a complete set of electron scattering cross sections is essential for predicting the performance of fluoronitriles in plasma reactors, industrial gas discharges, gas insulated transmission line (GIL), and gas insulated switchgear (GIS). Only a handful of electron

interaction investigations have been conducted with fluoronitriles, and a literature survey reveals that there are no results for $Q_{el}$, elastic cross sections, or, $Q_T$ total cross sections.

Number of studies have been undertaken on the gases $C_4F_7N$ and $C_3F_5N$, with the majority of them focusing on their insulating properties under various environmental conditions. There have been few investigations on microscopic parameters such as ionization cross sections after electron collision. The ionization cross sections ($Q_{ion}$) is an important quantity in understanding electron avalanche and gas breakdown mechanisms.

A study of the literature shows that results of $Q_{el}$, elastic cross - section, and $Q_T$, total cross - section, do not exists, and just a few electron impact investigations with fluoronitriles have been conducted (table 5.1). This is especially the case for information relevant to inelastic processes, such as calculating ionization probabilities.

This is the first attempt at identifying the cross sections for all potential excitations of $C_3F_5N$. We also want to point out that there have been no earlier research or experimental investigations on the elastic ($Q_{el}$) or total ($Q_T$) cross sections of these fluoronitriles. Due to their environmental significance and significance to plasma physics, fluoronitrile molecules are studied in depth here, from IP to 5 keV, to describe the probability of numerous molecular reactions occurring upon electron impact.

## 5.2 Literature Survey Of Fluoronitrile Compounds

In table 5.1, we discuss all these investigations carried out. Let us review the previous

Studies of the fluoronitiles as follows:

*Table 5.1 Previous research addressed the scattering of electrons by fluoronitriles*

| Molecules | Parameters | Impact Energy ($E_i$) | References |
|---|---|---|---|
| $C_3F_5N$ | $Q_{ion}$ | IP-1000eV | [11] |
| $C_4F_7N$ | $Q_{ion}$ | IP-1000eV | [11] |
| | $Q_{ion}$ | IP-2000eV | [9] |
| | $Q_{ion}$ | IP-100eV | [12] |
| | $Q_{inel}$, $Q_{ion}$, $\Sigma Q_{exc}$ | IP-5000eV | [13] |

## 5.3 Properties Of Fluoronitriles

Table 5.2 summarises the dielectric strengths and GWP of the molecules studied in relation to $SF_6$.

*Table 5.2 Comparison of the GWP and dielectric strength of $SF_6$, $C_3F_5N$ and $C_4F_7N$*

| Molecule | $E_r$ (rel. $SF_6$) | GWP |
|---|---|---|
| $C_3F_5N$ | 2 [14] | - |
| $C_4F_7N$ | 2.74 [9] | 2100 [9] |
| $SF_6$ | 1 | 23900 [15] |

Table 5.3 displays the properties of the fluoronitrile compounds that are used in estimations.

*Table 5.3 Target properties of $C_3F_5N$ and $C_4F_7N$*

| Molecule | IP(eV) | Polarizability ($cm^{-3}$) |
|---|---|---|
| $C_3F_5N$ | 15.20 [14] | 5.72 [16] |

| | | |
|---|---|---|
| $C_4F_7N$ | 15.10 [14] | 6.82 [16] |

Figure 5.1 depicts a schematic diagram of fluoronitrile compounds.

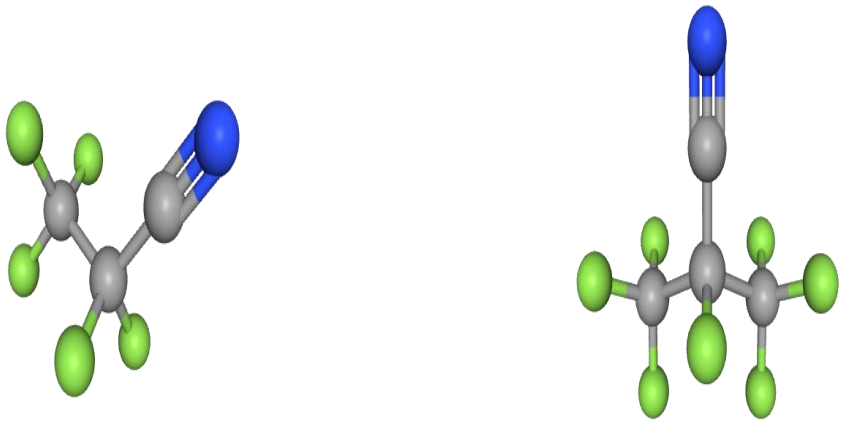

**$C_3F_5N$** **$C_4F_7N$**

**Figure 5.1 Diagrammatic representations of fluoronitrile molecules**
**(**https://pubchem.ncbi.nlm.nih.gov**)**

## 5.4 Total Cross Sections For Fluoronitriles

We investigated the electron interaction with two plasma-relevant compounds, including $C_3F_5N$ and $C_4F_7N$. We presented findings together with modest comparisons in two categories:

**(A) Inelastic cross sections:** Graphical findings from $Q_{inel}$, $Q_{ion}$, and $\Sigma Q_{exc}$ have been reported in this category. $Q_{ion}$'s ionization cross sections are calculated using the CSP-ic technique.

**(B) Total and elastic cross sections:** In this category, the graphical outcome of $Q_T$ and $Q_{el}$ has been reported.

### 5.4.1 Pentafluoropropionitrile

**(A) Inelastic processes**

As shown in figure 5.2, we will provide inelastic processes for Pentafluoropropionitrile molecules in this subsection and compare them with previous studies.

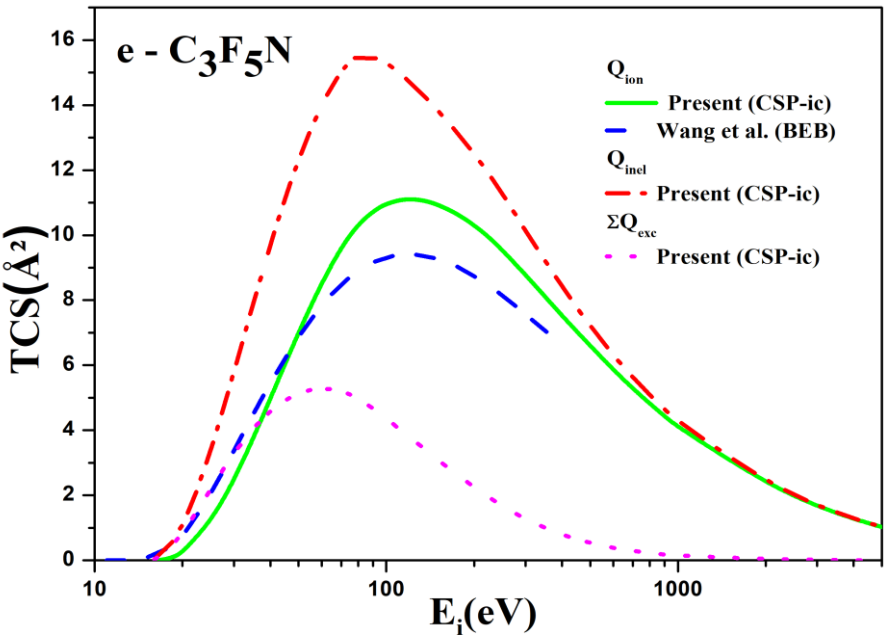


**Figure 5.2 Inelastic processes for Pentafluoropropionitrile**

**Solid: $Q_{ion}$ (Present); Dashed:** [11] **$Q_{ion}$ (BEB); Dash Dotted: $Q_{inel}$(Present); Dotted: $\Sigma Q_{exc}$(Present)**

As can be seen in Figure 5.2 that displays results of e- $C_3F_5N$, the upper most $Q_{inel}$ curve depicts total inelastic cross sections. We do not find any previous data of $Q_{inel}$.

The current $Q_{ion}$ for $C_3F_5N$ matches reasonably well with the BEB estimation of Wang et al. [14] across the whole energy range. Our $Q_{ion}$ values increase more slowly than the BEB data, that reported uncertainty of 10% [17–19]. There is no comparison in the literature to the curve at the bottom, denoted as $\Sigma Q_{exc.}$ which shows summed total excitation cross sections. $\Sigma Q_{exc}$ attain peak at 45eV.

**(B) Total and elastic cross-sections**

In figure 5.3, $Q_{el}$ and $Q_T$ are shown. The two theories applied to find cross-sections match well across the given energy range.

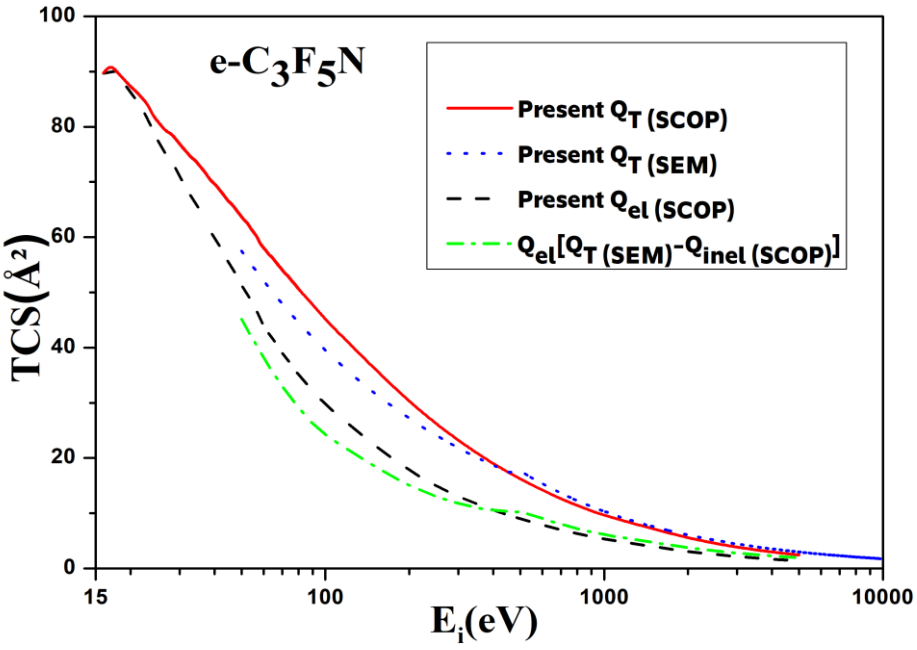


**Figure 5.3 Elastic processes for Pentafluoropropionitrile**

**Solid: $Q_T$(SCOP) (Present); Dotted: $Q_T$(SEM) (Present); Dashed: $Q_{el}$ (SCOP) (Present);Dash Dotted: $Q_{el}$ (SEM) (Present)**

Table 5.4 lists the computed TCS values for $C_3F_5N$.

***Table 5.4 Total cross-sections (Å²) for Pentafluoropropionitrile molecule***

| $E_i$ (eV) | $Q_{ion}$ | $Q_{el}$ | $Q_T$ |
|---|---|---|---|
| 16 | 0 | 89.715 | 89.744 |
| 20 | 0.248 | 86.141 | 87.252 |
| 30 | 2.455 | 71.099 | 76.891 |
| 40 | 4.975 | 60.053 | 69.732 |

| | | | |
|---|---|---|---|
| 50 | 6.999 | 51.414 | 63.719 |
| 60 | 8.509 | 44.084 | 58.07 |
| 70 | 9.598 | 39.048 | 54.066 |
| 80 | 10.304 | 35.111 | 50.625 |
| 90 | 10.717 | 32.241 | 47.884 |
| 100 | 10.959 | 29.408 | 44.986 |
| 200 | 10.299 | 17.235 | 29.907 |
| 300 | 8.78 | 12.956 | 23.1 |
| 400 | 7.536 | 10.539 | 18.943 |
| 500 | 6.6 | 9.016 | 16.216 |
| 600 | 5.874 | 7.899 | 14.21 |
| 700 | 5.292 | 6.991 | 12.615 |
| 800 | 4.828 | 6.338 | 11.425 |
| 900 | 4.436 | 5.793 | 10.436 |
| 1000 | 4.097 | 5.324 | 9.593 |
| 2000 | 2.367 | 2.994 | 5.401 |
| 3000 | 1.662 | 2.141 | 3.823 |
| 4000 | 1.28 | 1.686 | 2.977 |
| 5000 | 1.026 | 1.415 | 2.446 |

### 5.4.2 Heptafluorobutyronitrile

**(A) Inelastic Proceeses**

In figure 5.4 inelastic effects for $C_4F_7N$ are shown. That includes $Q_{inel}$, $Q_{ion}$ and $\Sigma Q_{exc}$ cross sections.

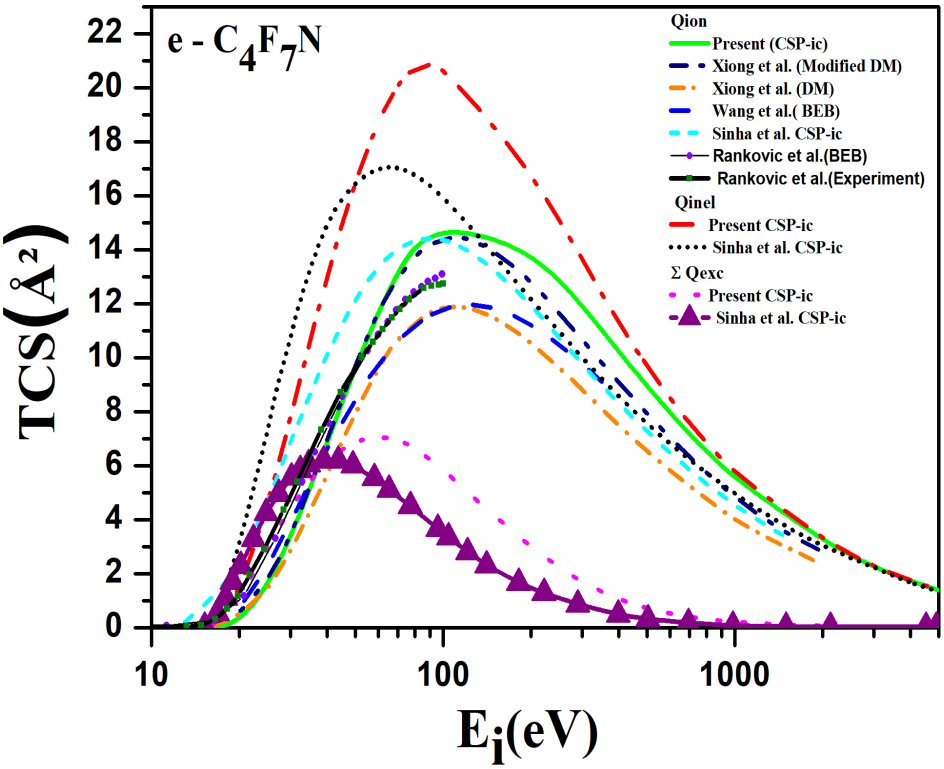


**Figure 5.4 Inelastic processes for $C_4F_7N$**

**Solid: $Q_{ion}$(Present); Dashed: Wang et al.,2019 $Q_{ion}$ (BEB); Dash Dot Dotted: Xiong et al.** [9]**$Q_{ion}$ (Modified DM); Short Dashed Dot: Xiong et al.** [9] **$Q_{ion}$ (DM); Short Dashed l: Sinha et al.** [13] **$Q_{ion}$ (CSP-ic); -●- Rankovic et al.** [12]**(BEB) $Q_{ion}$; -■- Rankovic et al.** [12]**(Experiment) $Q_{ion}$; Dash Dotted: Present $Q_{inel}$(Present); Short Dotted : Sinha et al.** [13] **$Q_{inel}$ (CSP-ic); Dotted:Present $\Sigma Q_{exc}$; -◀- line: Sinha et al.** [13] **$\Sigma Q_{exc}$ (CSP-ic)**

Figure 5.4 depicts the electron scattering cross sections for $C_4F_7N$. The magnitude of the cross sections given here for $Q_{inel}$ and $\Sigma Q_{exc}$ is larger than that of the results reported by Sinha et al. [13]. Sinha et al.'s [13] $Q_{ion}$ result is slightly left shifted. This difference may be due to the incorporation of nuclear charge into the calculation, which affects both the position and peak value, as Sinha et al. [13] have mentioned. The Modified DM results provided by Xiong et al. [9] are consistent with the present $Q_{ion}$ data. While showing reasonable agreement up to $Q_{ion}$'s peak, the BEB and DM results are lower for the higher energy levels. In addition to these

findings, the present CSP-ic result is in rather good agreement with the experimental data of the ionisation cross section by Rankovic et al. [12] at lower energies.

**(B) Elastic processes**

In this subsection, we will demonstrate the current $Q_{el}$ and $Q_T$ for fluoronitrile molecules by using figures 5.5. Figure 5.5 depicts $Q_{el}$ and $Q_T$. The two theories used to calculate cross-sections agree well over the specified energy range.

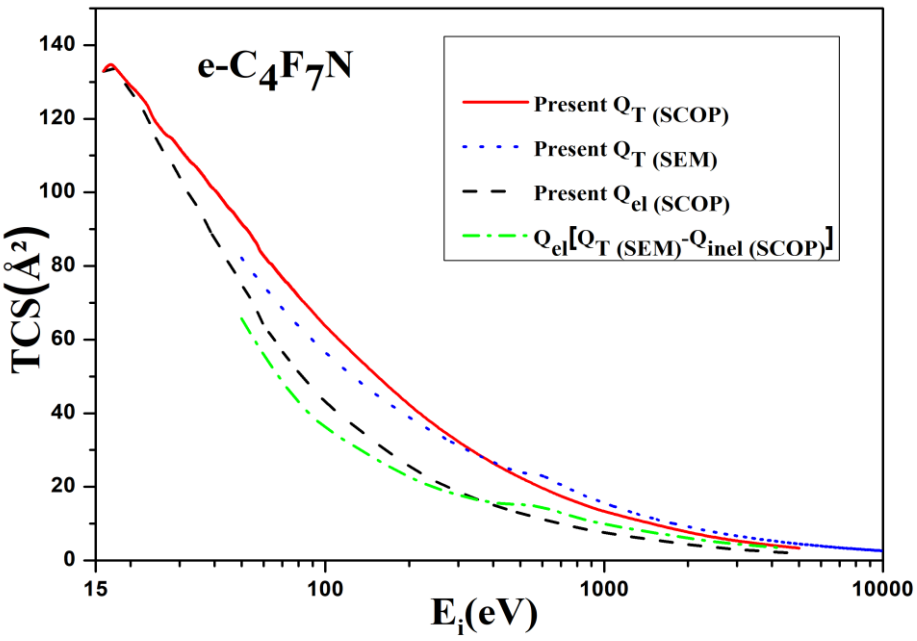


**Figure 5.5 Elastic processes for $C_4F_7N$**

**Solid: $Q_T$(SCOP)( Present); Dotted: $Q_T$(SEM) ( Present); Dashed: $Q_{el}$ (SCOP) ( Present);Dash Dotted: $Q_{el}$ (SEM) ( Present)**

Table 5.5 lists the computed TCS values for $C_4F_7N$.

Here we show SCOP and 2p-SEM results for $Q_T$ in figures 5.3 and 5.5 through the top curves for $C_3F_5N$ and $C_4F_7N$ respectively. $Q_T$ expresses the probability of all electron-induced molecular processes, and it finds use in a variety of modelling methodologies [20,21]. At higher energies, as expected, $Q_T$ decreases as a function of $\frac{1}{E_i}$ in accordance with the Born-Bethe trend. The reported $Q_T$ and $Q_{el}$ using recently developed 2p-SEM method gives excellent

agreement. This is the first effort to describe the $Q_{el}$ and $Q_T$ by two various methods upon electron impact for these key compounds that are crucial to environmental and plasma studies.

***Table 5.5 Total cross-sections (Å$^2$) for Heptafluorobutyronitrile molecule***

| $E_i$ (eV) | $Q_{ion}$ | $Q_{el}$ | $Q_T$ |
|---|---|---|---|
| 16 | 0 | 132.876 | 132.93 |
| 20 | 0.362 | 127.318 | 128.862 |
| 30 | 3.412 | 104.133 | 111.957 |
| 40 | 6.859 | 87.856 | 100.847 |
| 50 | 9.617 | 75.1 | 91.571 |
| 60 | 11.659 | 64.104 | 82.805 |
| 70 | 13.127 | 56.782 | 76.847 |
| 80 | 13.999 | 51.041 | 71.746 |
| 90 | 14.49 | 46.89 | 67.771 |
| 100 | 14.95 | 42.576 | 63.36 |
| 200 | 14.048 | 24.691 | 41.66 |
| 300 | 11.952 | 18.521 | 32.13 |
| 400 | 10.24 | 15.003 | 26.287 |
| 500 | 8.962 | 12.817 | 22.493 |
| 600 | 7.969 | 11.223 | 19.71 |
| 700 | 7.168 | 9.897 | 17.46 |
| 800 | 6.545 | 8.977 | 15.822 |

| | | | |
|---|---|---|---|
| 900 | 6.011 | 8.193 | 14.445 |
| 1000 | 5.555 | 7.522 | 13.274 |
| 2000 | 3.199 | 4.215 | 7.461 |
| 3000 | 2.248 | 3.004 | 5.272 |
| 4000 | 1.737 | 2.367 | 4.112 |
| 5000 | 1.388 | 1.975 | 3.371 |

Using the SCOP approach, we are able to compute $Q_{el}$ in addition to $Q_{inel}$ in the following manner:

$$Q_T(E_i) = Q_{el}(E_i) + Q_{inel}(E_i)$$

The $Q_T$ for fluoronitrile molecules is indicated in these graphs using the top curves. $Q_T$ is a notation that expresses the probability that all electron-induced molecular processes will take place, and it finds use in a variety of methodologies [20,22]. At higher energies, as can be observed, $Q_T$ decreases as a function of $\frac{lnE_i}{E_i}$ in accordance with the Born-Bethe trend. The $Q_{el}$ for fluoronitrile molecules are represented by the bottom curves in the above two figures. The reported $Q_T$ and $Q_{el}$ using developed 2p-SEM method gives excellent agreement at higher energies. Hence, this is the first effort to describe the $Q_{el}$ and $Q_T$ by two various method upon electron impact for these key compounds that are crucial to environmental and plasma studies.

## 5.5 Various Correlations: Prediction Of Polarizability And Dielectric Constant

The SCOP technique discusses how the interactions between electrons and charged cloud of the molecule takes place and allows for an estimation of the possibility of various electron-assisted chemical processes. Table 5.6 shows the polarizability and other properties of $C_3F_5N$, $C_4F_7N$, and perfluoroketone (PFK) ($C_xF_{2x}O$, x=5-6) [23] molecules that are either available in

the literature or are expected to be studied in this work. The data and correlations may be used to calculate the polarizability of fluoroketone and fluoronitrile. The total number of electrons determines the size of the molecular cloud ($n_e$).

***Table 5.6 Molecular properties and predicted α***

| Target | $n_e$ | Ionization Potential (eV) | Polarizability ($10^{-24}$cm$^{-3}$) | | |
|---|---|---|---|---|---|
| | | | Present | Estimated | Found at www.chemspider.com |
| $C_3F_5N$ | 70 | 15.20 [11] | 5.72 [16] | 5.97 | 6.6 (deviation 10%) |
| $C_4F_7N$ | 94 | 15.10[12] | 6.82 [16] | 7.60 | 8.5 (deviation 11%) |
| $C_5F_{10}O$ | 128 | 12.02 [24] | 8.83 [25] | 9.84 | 10.6 (deviation 7.1%) |
| $C_6F_{12}O$ | 152 | 11.41 [26] | 11.44 [27] | 12.54 | 12.6 (deviation 0.4 %) |

In figure 5.6 the behaviour of $Q_{ion}$ (max) with respect to number of electrons of molecules is shown.

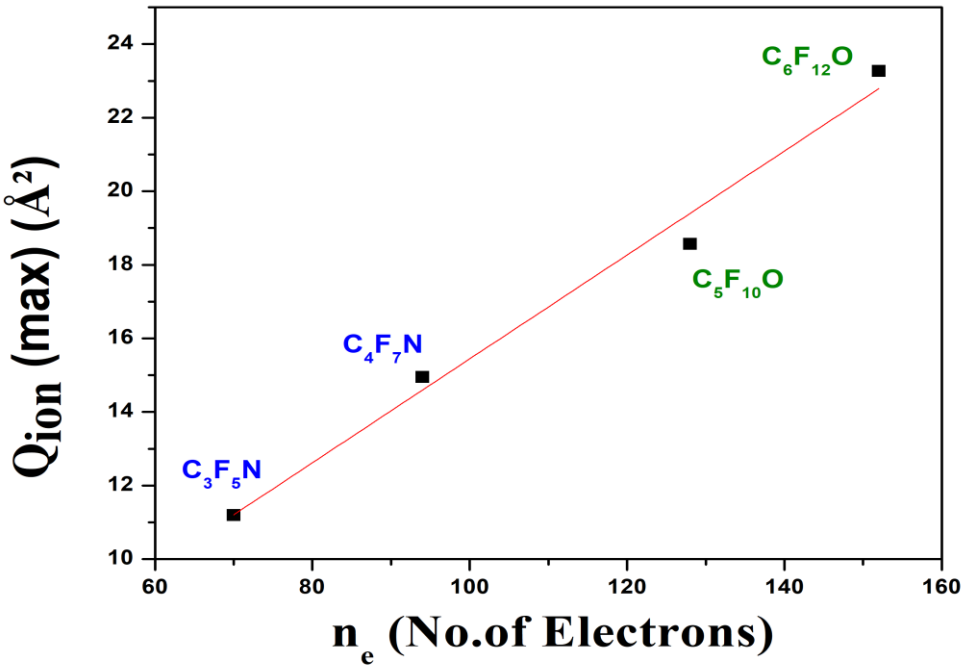


**Figure 5.6 Variation of $Q_{ion}$(max) with $n_e$**

The size of the molecular cloud, defined by the number of electrons, $n_e$, is significant for the peak of $Q_{ion}$ of each molecule. When the charge cloud expands in size, the orders of magnitude of impact energy-specific cross sections increase. $Q_{ion}$ depends on the initial ionization potential, which does not vary considerably for extremely big molecules, in addition to the target cloud size (table 5.6). As a result, a linear connection between $Q_{ion}$ (max) and $n_e$ is seen (figure 5.6).

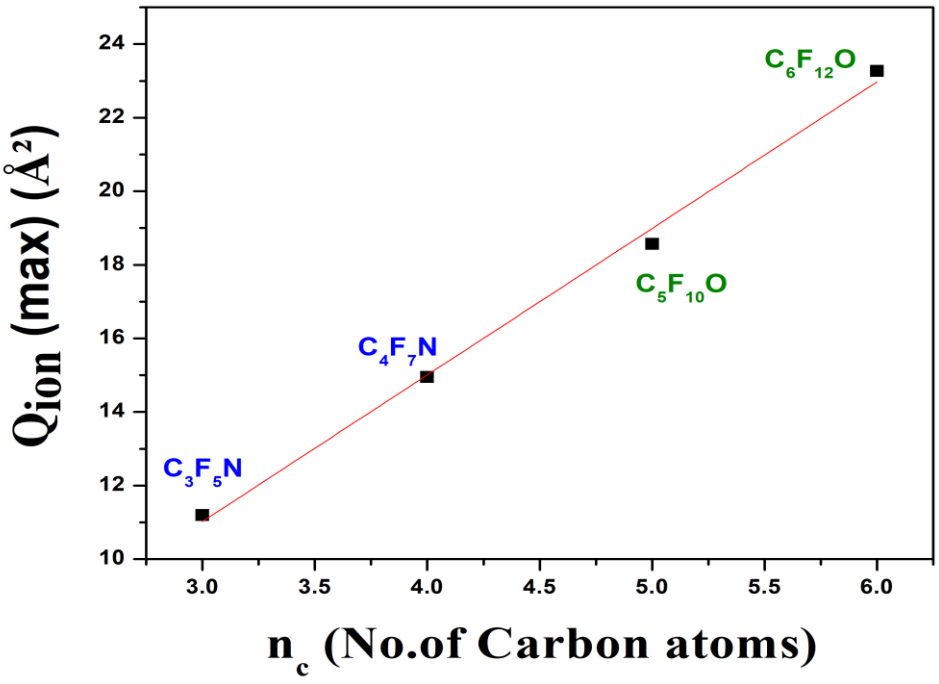


**Figure 5.7 Variation of $Q_{ion}$(max) with $n_c$**

Figure 5.7 shows a similar trend for $Q_{ion}$ (max) with the number of C (carbon) atoms present in the target for fluoroketones and fluoronitriles. These relationships, together with some simple extrapolation, can be used to predict the $Q_{ion}$ (max) of such large molecules.

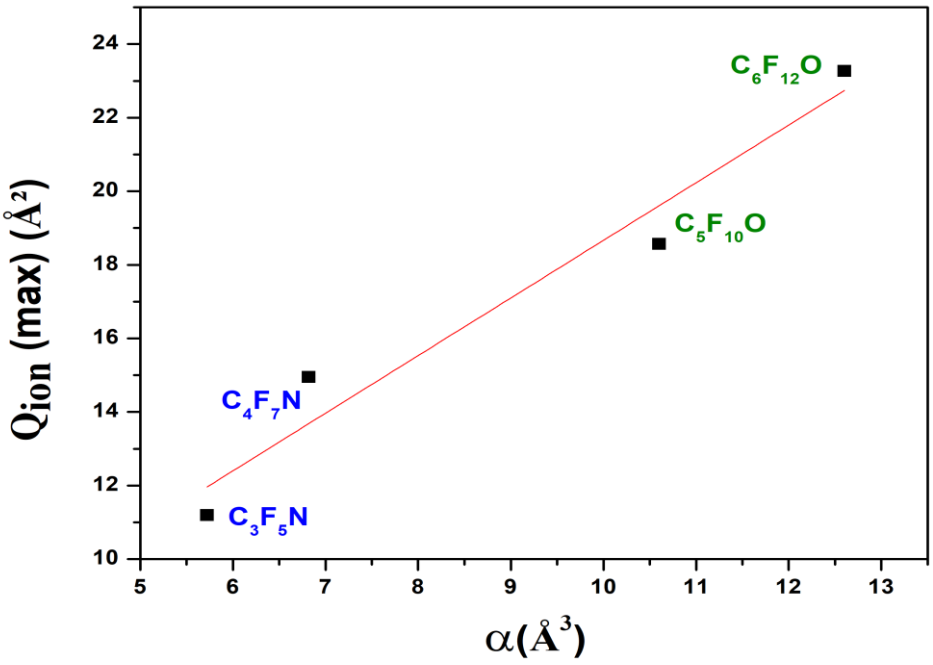


**Figure 5.8 Variation of $Q_{ion}$(max) with α**

In figure 5.9, we established a linear relation between $Q_{ion}$(max) and ε. With the help of this, we can estimate the dielectric constant for the series of molecules from $Q_{ion}$ values. We can also predict $Q_{ion}$ from dielectric constant. Our findings confirm the linear relationship between $Q_{ion}$ (max) and polarizability, as reported by Bart et al. [28], through which we can predict polarizability for similar compounds like $C_3F_5N$, $C_4F_7N$, $C_5F_{10}O$ and $C_6F_{12}O$. In table 5.6, we can see an excellent matching between the predicted and the computed values, up to 95.18% for $C_3F_5N$, 90% for $C_4F_7N$ and for, $C_5F_{10}O$, $C_6F_{12}O$ it is about 92.80% and 99.50% respectively. Table 5.6 shows various properties including polarizability of $C_3F_5N$, $C_4F_7N$, and perfluoroketone (PFK) ($C_XF_{2X}O$, x=5-6) [23] molecules. The data and correlations can be used to predict the polarizability of fluoroketones and fluoronitriles. The total number of electrons ($n_e$) decides the dimension of the molecular cloud

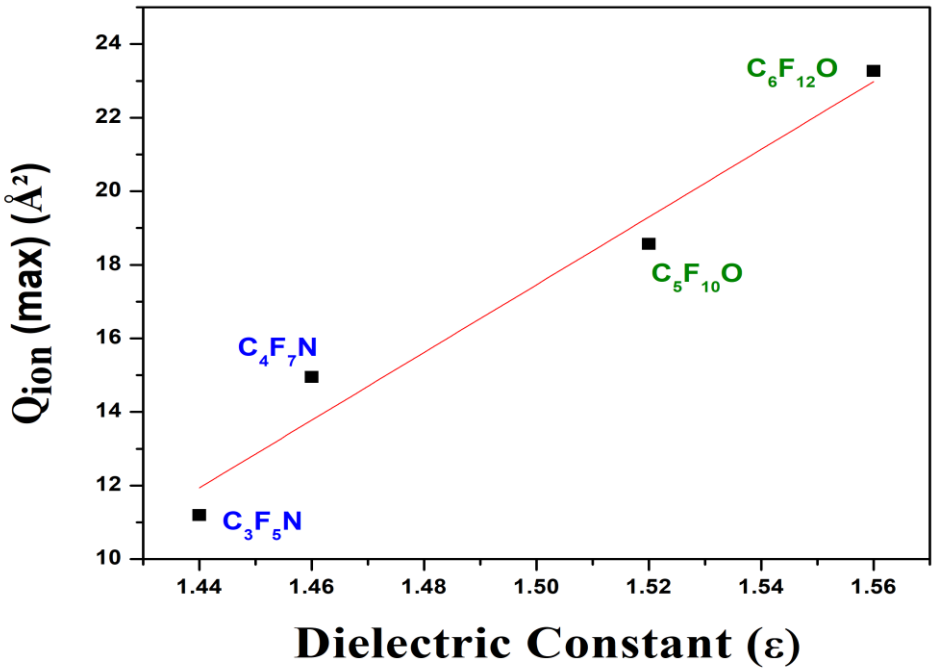


**Figure 5.9 Variation of $Q_{ion}$(max) with ε**

In table 5.7, we report number density and computed dielectric constant using polarizability for $C_3F_5N$ and $C_4F_7N$.

***Table 5.7 Calculated number density N and dielectric constant ε***

| Target | Polarizability, α ($10^{-24}cm^{-3}$) | Density of material, ρ $g/cm^3$ | Molar mass, M $g/mol$ | Calculated Number Density, N $molecules/cm^3$ | Calculated Dielectric Constant, ε |
|---|---|---|---|---|---|
| $C_3F_5N$ | 5.72 [16] | 1.5 [29] | 145.03 [29] | $6.2*10^{21}$ | 1.52 |
| $C_4F_7N$ | 6.82 [16] | 1.5±0.1 [29] | 195.03 [29] | $4.6*10^{21}$ | 1.45 |

The Clausius-Mossotti equation yields a linear connection between polarizability and dielectric constant. We may assume a linear relationship between $Q_{ion}$ (max) and the dielectric constant since there is a linear relationship between $Q_{ion}$ (max) and polarizability [28], as shown in

figure 5.8. Figure 5.9 depicts this property for the molecules under consideration. Consequently, the present research of cross section computation upon electron impact can aid in predicting dielectric constant for any electrically conductive substance.

According to J. C. Devins' research, fluoro-nitrile organic gases such as $C_3F_5N$ and $C_4F_7N$ can have double the electric strength of $SF_6$ [30]. When compared to pure epoxy resin, the electrical characteristics of a composite material consisting of $C_3F_5N$ and epoxy resin demonstrated better dielectric strength and thermal stability. In the design and optimisation of this composite material, the dielectric constant of $C_3F_5N$ was employed as a crucial parameter [31].

The dielectric characteristics of $C_4F_7N$ suggest that it might be used as a high-performance insulating gas in power equipment. The dielectric constant was found to be much larger than that of $SF_6$, a commonly used insulating gas, indicating that $C_4F_7N$ might be a potential option for use in power equipment [32,33].

## 5.6 Chapter Summary

We report quantified probabilities of various electron assisted molecular processes for applied fluoronitriles $C_3F_5N$ and $C_4F_7N$ for wide impact energies (IP to 5 keV). We performed calculations for $Q_{el}$, $Q_{inel}$, and $Q_T$ using the SCOP formalism, obtained $Q_{ion}$ and $\Sigma\Sigma Q_{exc}$ through CSP-ic method and displayed results graphically in figures 5.2 – 5.5 along with available comparison. Present $Q_{ion}$ agrees reasonably well with adjusted DM data [9] and BEB [11] for these compounds (figure 5.2 and 5.3). Since there is no previous data on $Q_{el}$ and $Q_T$ we have compared present $Q_{el}$ and $Q_T$ computed through SCOP with newly developed 2 parameter semi empirical method (2p-SEM) in figure 5.4 and 5.5. This new method is applicable for large molecules ($55<Z<95$) and over a wide energy range 50 eV$<E_i<$5000 eV. We find excellent agreement throughout the energy range of investigation for $Q_{el}$ and $Q_T$.

We also verified the sensitivity of $Q_{ion}$ to size of the molecule ($n_e$) as well as total number of carbon atoms ($n_e$ ) and observed a linear relationship $Q_{ion}$ (max) with them (figure 5.6 and 5.7). We found a linear correlation between $Q_{ion}$ (max) and polarizability shown in figure 5.8 as expected by Bart et al. [34]. When we compared our predictions for the dipole polarizability of $C_3F_5N$, $C_4F_7N$, $C_2F_4O$, $C_5F_{10}O$, and $C_6F_{12}O$ to those computed using

www.chemspider.com, we found that our predictions were in excellent agreement with those of the latter as mentioned in table 5.6.

These two significant environmental and plasma-relevant compounds, $C_3F_5N$ and $C_4F_7N$, have an exceptionally greater dielectric strength and lower GWP, making them appealing for commercial prospects and effective alternative for $SF_6$. For these applied molecules we also found number density N and reported dielectric constant ε using molecular polarizability and observed a linear relation between $Q_{ion}$ (max) and the dielectric constant of the system as shown in figure 5.9. Thus the current study of cross section calculations upon electron impact can help predict dielectric constant for any materials of electrical applications.

While this work is the maiden report of $\Sigma Q_{exc}$ and $Q_{inel}$ for $C_3F_5N$, it is the first study of $Q_{el}$ and $Q_T$ for both $C_3F_5N$ and $C_4F_7N$ using SCOP as well 2p-SEM methods. Reported theoretical results in this work may encourage experimentalists to embark on similar projects.

## 5.7 Bibliography


[1] B. Zhang, M. Hao, Y. Yao, J. Xiong, X. Li, A. B. Murphy, N. Sinha, B. Antony, and H. B. Ambalampitiya, *Determination and Assessment of a Complete and Self-Consistent Electron-Neutral Collision Cross-Section Set for the C4F7N Molecule*, J Phys D Appl Phys **56**, 134001 (2023).

[2] J. Zhang, N. Sinha, M. Jiang, H. Wang, Y. Li, B. Antony, and C. Liu, *DC Breakdown Characteristics of CFN/CO Mixtures with Particle-in-Cell Simulation*, IEEE Transactions on Dielectrics and Electrical Insulation **29**, 1005 (2022).

[3] M. Flynn, J. Agan, A. Neuber, and J. Stephens, *Generation and Optimization of Cross-Sections for Electron-C4F7N Collisions*, J Phys D Appl Phys **56**, 485207 (2023).

[4] X. Zhang, Y. Li, S. Xiao, J. Tang, S. Tian, and Z. Deng, *Decomposition Mechanism of C5F10O: An Environmentally Friendly Insulation Medium*, Environ Sci Technol **51**, 10127 (2017).

[5] M. Vinodkumar, H. Bhutadia, C. Limbachiya, and K. N. Joshipura, *Electron Impact Total Ionization Cross Sections for H2S, PH3, HCHO and HCOOH*, Int J Mass Spectrom **308**, 35 (2011).

[6] K. N. Joshipura, B. G. Vaishnav, and C. G. Limbachiya, *Ionization and Excitation of Some Atomic Targets and Metal Oxides by Electron Impact*, Pramana - Journal of Physics **66**, 403 (2006).

[7] C. Limbachiya, M. Vinodkumar, M. Swadia, K. N. Joshipura, and N. Mason, *Electron-Impact Total Cross Sections for Inelastic Processes for Furan, Tetrahydrofuran and 2,5-Dimethylfuran*, Mol Phys **113**, 55 (2015).

[8] Y. K. Kim, W. Hwang, N. M. Weinberger, M. A. Ali, and M. E. Rudd, *Electron-Impact Ionization Cross Sections of Atmospheric Molecules*, Journal of Chemical Physics **106**, 1026 (1997).

[9] J. Xiong, X. Li, J. Wu, X. Guo, and H. Zhao, *Calculations of Total Electron-Impact Ionization Cross Sections for Fluoroketone C5F10O and Fluoronitrile C4F7N Using Modified Deutsch-Märk Formula*, J Phys D Appl Phys **50**, 2 (2017).

[10] D. Prajapati, H. Yadav, P. C. Vinodkumar, C. Limbachiya, A. Dora, and M. Vinodkumar, *Computation of Electron Impact Scattering Studies on Benzene*, The European Physical Journal D 2018 72:12 **72**, 1 (2018).

[11] F. Wang, Q. Dun, S. Chen, L. Zhong, X. Fan, and L. L. Li, *Calculations of Total Electron Impact Ionization Cross Sections for Fluoroketone and Fluoronitrile*, IEEE Transactions on Dielectrics and Electrical Insulation **26**, 1693 (2019).

[12] M. Ranković, J. Chalabala, M. Zawadzki, J. Kočišek, P. Slavíček, and J. Fedor, *Dissociative Ionization Dynamics of Dielectric Gas C3F7CN*, Physical Chemistry Chemical Physics **21**, 16451 (2019).

[13] N. Sinha, V. M. Patel, and B. Antony, *Ionization Cross Sections for Plasma Relevant Molecules*, Journal of Physics B: Atomic, Molecular and Optical Physics **53**, (2020).

[14] F. Wang, Q. Dun, S. Chen, L. Zhong, X. Fan, and L. L. Li, *Calculations of Total Electron Impact Ionization Cross Sections for Fluoroketone and Fluoronitrile*, IEEE Transactions on Dielectrics and Electrical Insulation **26**, 1693 (2019).

[15] S. Tian, X. Zhang, S. Xiao, J. Zhang, Q. Chen, and Y. Li, *Application of C6F12O/CO2 Mixture in 10 KV Medium-voltage Switchgear*, Wiley Online LibraryS Tian, X Zhang, S Xiao, J Zhang, Q Chen, Y LiIET Science, Measurement & Technology, 2019•Wiley Online Library **13**, 1225 (2019).

[16] Y. Wu, C. Wang, H. Sun, A. B. Murphy, M. Rong, F. Yang, Z. Chen, C. Niu, and X. Wang, *Properties of C4F7N-CO2 Thermal Plasmas: Thermodynamic Properties, Transport Coefficients and Emission Coefficients*, J Phys D Appl Phys **51**, (2018).

[17] C. Limbachiya, M. Vinodkumar, M. Swadia, and A. Barot, *Electron Impact Total Cross Section Calculations for CH 3SH (Methanethiol) from Threshold to 5 KeV*, Mol Phys **112**, 101 (2014).

[18] Y. K. Kim and P. M. Stone, *Ionization of Boron, Aluminum, Gallium, and Indium by Electron Impact*, Phys Rev A **64**, 11 (2001).

[19] Y. K. Kim and J. P. Desclaux, *Ionization of Carbon, Nitrogen, and Oxygen by Electron Impact*, Phys Rev A **66**, 127081 (2002).

[20] M. Vinodkumar, C. Limbachiya, A. Barot, and N. Mason, *Computation of Electron-Impact Rotationally Elastic Total Cross Sections for Methanol over an Extensive Range of Impact Energy (0.1 - 2000 EV)*, Phys Rev A **87**, 1 (2013).

[21] M. Swadia, R. Bhavsar, Y. Thakar, M. Vinodkumar, and C. Limbachiy, *Electron-Driven Processes for Furan, Tetrahydrofuran and 2, 5-Dimethylfuran*, Mol Phys **115**, 2521 (2017).

[22] M. Vinodkumar, C. Limbachiya, H. Desai, and P. C. Vinodkumar, *Electron-Impact Total Cross Sections for Phosphorous Triflouride*, Phys Rev A **89**, 1 (2014).

[23] N. Thakkar, M. Swadia, M. Vinodkumar, N. Mason, and C. Limbachiya, *Electron Induced Elastic and Inelastic Processes for Perfluoroketone (PFK) Molecules*, Plasma Sources Sci Technol **30**, (2021).

[24] L. Zhong, J. Wang, X. Wang, and M. Rong, *Calculation of Electron-Impact Ionization Cross Sections of Perfluoroketone (PFK) Molecules CxF2xO (x = 1-5) Based on Binary-Encounter-Bethe (BEB) and Deutsch-Märk (DM) Methods*, Plasma Sources Sci Technol **27**, (2018).

[25] Y. Wu, C. Wang, H. Sun, M. Rong, A. B. Murphy, T. Li, J. Zhong, Z. Chen, F. Yang, and C. Niu, *Evaluation of SF6-Alternative Gas C5-PFK Based on Arc Extinguishing Performance and Electric Strength*, J Phys D Appl Phys **50**, (2017).

[26] X. Zhang, S. Tian, S. Xiao, Z. Deng, Y. Li, and J. Tang, *Insulation Strength and Decomposition Characteristics of a C6F12O and N2 Gas Mixture*, Energies (Basel) **10**, (2017).

[27] X. Yu, H. Hou, and B. Wang, *Prediction on Dielectric Strength and Boiling Point of Gaseous Molecules for Replacement of SF6*, J Comput Chem **38**, 721 (2017).

[28] M. Bart, P. W. Harland, J. E. Hudson, and C. Vallance, *Absolute Total Electron Impact Ionization Cross-Sections for Perfluorinated Hydrocarbons and Small Halocarbons*, Physical Chemistry Chemical Physics **3**, 800 (2001).

[29] D. P, *CRC Handbook of Chemistry and Physics*, Vol. 268 (CRC Press, 1992).

[30] J. Jiao, D. Xiao, X. Zhao, and Y. Deng, *Analysis of the Molecules Structure and Vertical Electron Affinity of Organic Gas Impact on Electric Strength*, Plasma Science and Technology **18**, 554 (2016).

[31] R. E. Wootton et al., Gases Superior To Sf6 for Insulation and Interruption., 1982.

[32] R. Qiu, W. Zhou, Y. Zheng, S. Hu, H. Li, and J. Yu, *A Simulation Research on Diffusion Processes of Discharging Decomposition Products of C4F7N/CO2 in Gas Insulated Transmission Lines*, 7th IEEE International Conference on High Voltage Engineering and Application, ICHVE 2020 - Proceedings 20 (2020).

[33] N. Tang, L. Chen, B. Zhang, and X. Li, *Experimental and Theoretical Exploration of C4F7N Gas Decomposition under Partial Discharge*, 7th IEEE International Conference on High Voltage Engineering and Application, ICHVE 2020 - Proceedings 4 (2020).

[34] J. N. Bull, P. W. Harland, and C. Vallance, *Absolute Total Electron Impact Ionization Cross-Sections for Many-Atom Organic and Halocarbon Species*, Journal of Physical Chemistry A **116**, 767 (2012).